Mechanics of Composite Materials, Vol. 50, No. 3, July, 2014 (Russian Original Vol. 50, No. 3, May-June, 2014)

MODELING LARGE DEFORMATIONS OF FIBROUS BODIES OF REVOLUTION BASED ON APPLIED AND CARCASS THEORIES

2. REDUCTION BY PRESSURE

V. M. Akhundov*

Keywords: *single- and two-level theories, fibrous prismatic and cylindrical bodies, unidirectional reinforcement, reduction by pressure, large deformations*

On the basis of single-level applied and two-level carcass theories, large deformations of regularly fiber-reinforced bodies are examined. Results of solution of the problem on pressure-reduction of unidirectionally reinforced prismatic and cylindrical bodies rigidly fixed at their end faces, whose matrix and fibers are made of compressible materials, are presented. The results obtained by both the theories are compared, and the possibility of using, under the conditions considered, solely the carcass theory in investigating pressurt-reduced bodies highly filled with fibers is clarified.

Introduction

In [1], solutions of the problems on butt-end torsion of a thick-walled cylinder with an axial reinforcement scheme and a toroidal body with a meridional arrangement of fibers are given. The problems were solved according to the applied [2] and carcass [3, 4] theories of fibrous materials and media under large deformations. In the present report, which is based on the above-mentioned approaches, solutions to the problems on compression of prismatic and cylindrical bodies with transverse and axial arrangements of fibers, respectively, are presented.

The numerical realizations of the approaches using the applied and carcass theories are described in [1]. We should note that, in the material model according to the applied theory, the macroscopic stresses are considered to be additively

National Metallurgical Academy of Ukraine, Dnepropetrovsk, Ukraine
*Corresponding author; e-mail: akhundov@ua.fm

Translated from Mekhanika Kompozitnykh Materialov, Vol. 50, No. 3, pp. 467-476 , May-June, 2014. Original article submitted March 3, 2014.

caused by stresses in the matrix and the forces in fibers of the reinforced material [2], whereas in that according to the carcass theory, the stresses are found from internal fields of the nodal blocks representing the material of the medium with account of curvings and breaks of the material plane (block face) on which stresses are determined [3, 4]. The applied theory is intended for calculating weakly reinforced bodies, whereas the carcass one can be used at any content of fibers. Investigation results indicate that, if during deformation of a body, fibers tend to arrange along the lines of greatest changes in material lengths in it, the applied theory can be employed at a high content of fibers, too (see [1]).

As in [1], the applied theory is realized on the basis of the finite-difference method with the use of finite-difference relations of the second order of accuracy for approximating the derivatives of basic quantities in terms of coordinate variables [5]. The numerical realization of the macromechanical level of the carcass theory is also based on the finite-difference method, with employment of finite-difference relations of the same order of accuracy. The microboundary-value problems for the nodal blocks of material of the body were solved by the method of local variations [6], with the use of approximation by isoparametric finite elements [7] and a technique for preventing the dead-end situations of "lockout" of numerical realization of the method [8].

We used a mesh of nodal blocks with their geometrical centers coinciding with nodal points of the discrete scheme of realization of the applied theory. In this case, the results obtained at the macromechanical level of solution of the problem by using the carcass theory can be correctly compared with those obtained by the applied theory. More detailed information on the numerical realizations according to the applied and carcass theories of the problems to be solved is given in [1].

The macroscopic quantities related to a body in a deformed state are marked by "^"; the quantities related to the matrix and fibers are designated by the subscripts "m" and "f", respectively.

1. Reduction by Pressure of a Rectangular Prism with a Transverse Reinforcement Scheme

Figure 1 shows the scheme of a long rectangular prism subjected to a reduction pressure on its lower and upper faces. A mesh of the nodal blocks of the macromechanical level of analysis of a prism is presented, for which the boundary-value problems of micromechanical level are solved. The prism is rigidly fixed on the lateral faces. The reinforcing fibers are packed squarely, and their axial lines lie in cross sections of the prism in parallel to the long side of cross section. The side lengths of cross section of the prism are $h = 200$ and $l = 400$ mm. The diameter of fibers $d_f = 0.7$ mm, their arrangement density $i_f = 1$ mm^{-2}, and the reinforcement ratio $k_{\rm f} = i_{\rm f}\pi d_{\rm f}^2/4 = 0.3848$.

The matrix material was described by the three-constant Levinson–Burgess potential [9] ($E_{\rm m} = 4$ MPa, $\nu_{\rm m} = 0.46$, and $\beta_m = 1$); the fiber material was modeled by the two-constant Blatz potential [10] ($E_{\rm f} = 36$ MPa and $\nu_{\rm f} = 0.4$). With the given low-modulus material of fibers, under the compressive strain of the reinforced body examined, their round transverse cross sections are transformed considerably. This may occur for some types of polyurethane fibers [11].

Solution of the problem at the macromechanical level was carried out under the conditions of a macroscopically plane deformation, when the parameters of macroscopic state of the deformed prism do not vary along its length. As the base system of Lagrange coordinates $\hat{\theta}^1$, $\hat{\theta}^2$, and $\hat{\theta}^3$, Cartesian coordinates were used, which, in the reference configurations of the prism, are designated by x_1, x_2, and x_3 (the reference system). The axes of the coordinate system are directed along edges of the prism: x_1 — along the longer side of cross section (along fiber axes), x_2 — along the axial line of the prism, and x_3 — along the height of cross section.

The convergence of solution by the carcass theory at the macromechanical level accurate to 1% was ensured by employing up to 41 rows of material blocks for the left (or right) half of the prism across its width and height. The accuracy of solution of the microboundary-value problems allowing one to calculate macrostresses with an error of 0.1% was achieved by using up to 31 × 31 nodal points for nodal blocks in the faces transverse to fibers (for more detail, see [12]). (The macrostresses, having an integral character with respect to internal fields, are calculated more precisely than the internal fields.)

The macrostrain of reinforced material of the prism obeys the conditions $\hat{\lambda}_2 = 1$ and $\widehat{\omega}_{12} = \widehat{\omega}_{23} = \pi/2$ (the subscripts 1 and 3 denote directions along the width and height of the prism, while the subscript 2 — the direction along it).

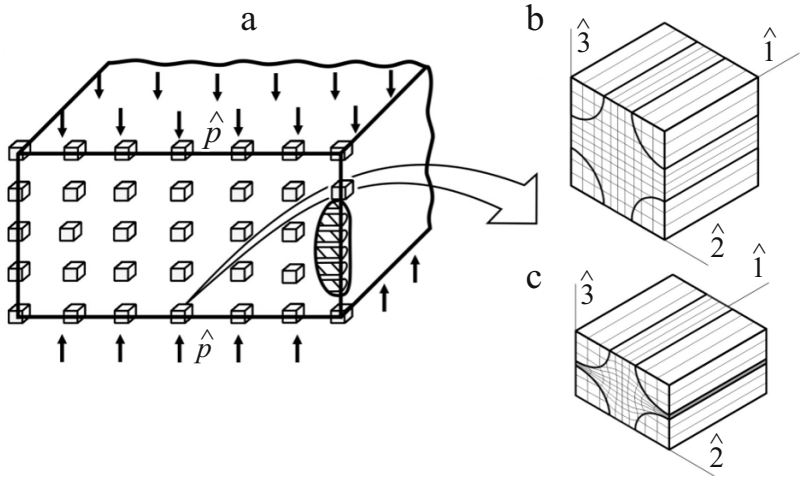

Fig. 1. A rectangular prism rigidly fixed on its lateral faces and reduced by a pressure applied to its lower and upper faces, with nodal blocks of the finite-difference scheme at the macromechanical level of analysis (a) and configurations of a block with the finite-element scheme at the micromechanical level of analysis in the reference state (b) and in the deformed configuration at $\hat{p} = 11$ MPa (c). Explanations in the text.

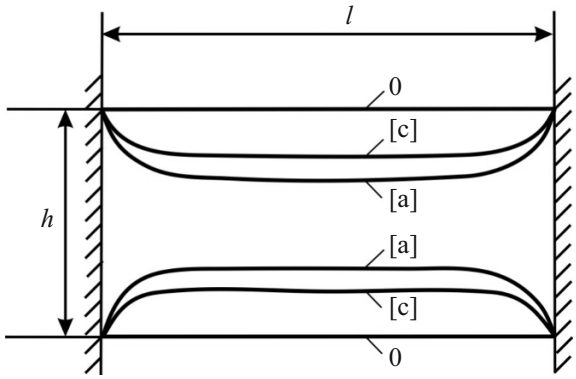

Fig. 2. Cross section of the prism in the reference state (0) and in its deformed configuration calculated by the carcass [c] and applied [a] theories at the content of fibers $k_f = 0.3848$ and pressure $\hat{p} = 11$ MPa.

Figure 1 also shows configurations of the nodal block of material at the center of the lower face of the prism in the initial and deformed states at a pressure $\hat{p}$ = 11 MPa. The configuration of the block is characterized by the macroscopic stretch ratio along fibers $\hat{\lambda}_1$ = 1.038, the normal reduction $\hat{\lambda}_3$ = 0.593, and the macrocoordinate angle $\hat{\omega}_{13} = \pi / 2$. We should note that the cross section of reinforcing fibers undergoes a considerable transformation (see Fig. 1c) — it becomes elliptic with the ratio between the horizontal (large) and vertical (small) axes $\hat{d}_{\mathrm{fa}} / \hat{d}_{\mathrm{fb}}$ = 0.724/0.551 = 1.314. The stretch ratio of the axial line of fiber $\hat{\lambda}_{\mathrm{f}}$ = 1.038 (in the case of unidirectional reinforcement, it coincides with the macroscopic stretch ratio $\hat{\lambda}_1$ of reinforced material along the reinforcement direction). A considerable volumetric deformation of fibers is achieved owing to a rather high compressibility of their material ($\nu_{\mathrm{f}} = 0.4$).

Figure 2 illustrates the initial and deformed configurations of the prism calculated according to the carcass and applied theories at the pressure $\hat{p} = 11$ MPa. The applied theory does not take into account the finite cross sections of filaments, which is essential for the given problem. When the applied theory is used, the calculation error of macroscopic state of the prism is

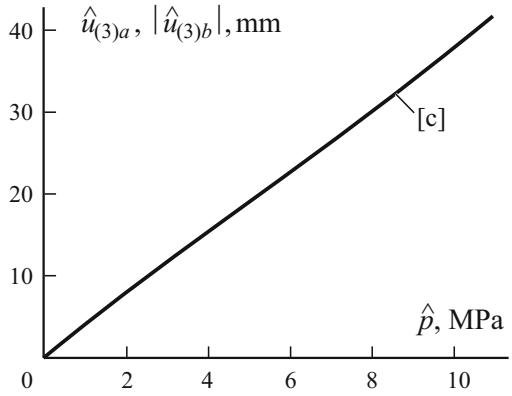

Fig. 3. Central deflections $\hat{u}_{(3)a}$ and $|\hat{u}_{(3)b}|$ of the lower and upper faces of the prism as functions of pressure $\hat{p}$ at $k_{\mathrm{f}} = 0.3848$, obtained by the carcass theory.

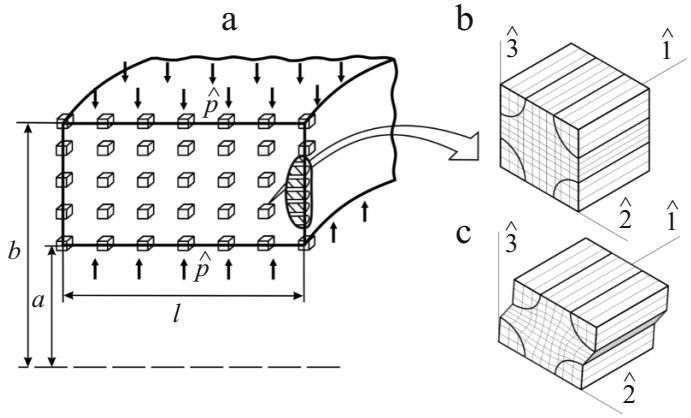

Fig. 4. A cylinder rigidly fixed at its butt ends and reduced by a pressure applied to its faces, with nodal blocks of the finite-difference scheme at the macromechanical level of analysis (a) and configurations of a block with the finite-element scheme at the micromechanical level of analysis in the reference state (b) and in the deformed configuration at $\hat{p} = 9$ MPa (c). Explanations in the text.

characterized by the ratio $\hat{u}^{[a]}_{(3)a} / \hat{u}^{[c]}_{(3)a} = 61.5/41.1 = 1.50$ between the greatest deflections of the lower face of the prism found by the applied and carcass theories. Figure 3 shows the deformation characteristic of the prism calculated by the carcass theory. The characteristic is the relation between the deflection of the lower face and the modulus of deflection of the upper face at the center of the prism, $\hat{u}_{(3)a}$ and $|\hat{u}_{(3)b}|$, as a function of the reduction pressure $\hat{p}$. The relation is almost linear on the range of pressures $0 \le \hat{p} \le 11$ MPa.

2. Reduction Pressure of a Thick-Walled Cylinder with an Axial Reinforcement Scheme

Figure 4 presents the scheme of a cylinder reduced by identical pressures on its faces. The cylinder is rigidly fixed at its butt ends. The axial (meridional) section of the cylinder is the same as the cross section of the prism in the previous problem: the radii of inner and outer surfaces are a = 200 mm and b = 400 mm, and the cross-sectional width l = 400 mm. The axial lines of fibers lie along the meridional sections of the cylinder in parallel with cylinder axis. The fiber diameter is $d_f = 0.7$ mm. The spatial density of fiber arrangement obeys the dependence $i_{\mathrm{f}} = i_{\mathrm{f}0} a / r$, $i_{\mathrm{f}0} = 1$ mm^{-2}. Accordingly, the content of fibers

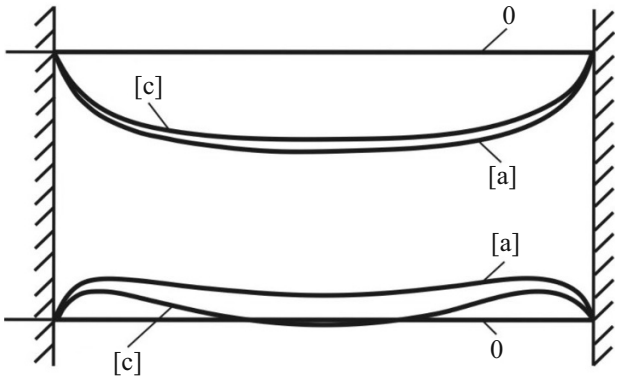

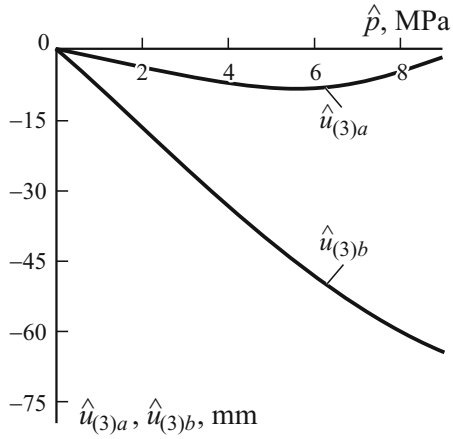

Fig. 5. Axial section of cylinder wall in the initial state (0) and its deformed configurations determined by the carcass [c] and applied [a] theories, at the content of fibers $k_{\rm f} = 0.3848\,a/r$ and pressure $\hat{p} = 9$ MPa.

Fig. 6. Central deflections $\hat{u}_{(3)a}$ and $\hat{u}_{(3)b}$ of the inner and outer surfaces of the cylinder as functions of pressure $\hat{p}$ at $k_{\rm f} = 0.3848\,a/r$, obtained according to the carcass theory.

varies from $k_{\rm f} = 0.3848$ at $r = a$ to $k_{\rm f} = 0.1924$ at $r = b$. The arrangement of fibers was assumed to fit the rectangular packing. Materials of the matrix and fibers were simulated in the same way as in the previous problem, at the same values of constants of the potentials used for their description.

As the base system of Lagrange coordinates, the system of cylindrical coordinates $\hat{\theta}^1$, $\hat{\theta}^2$, and $\hat{\theta}^3$ related to the inner face of the cylinder was adopted, where $\hat{\theta}^1$, $\hat{\theta}^2$, and $\hat{\theta}^2$ are the axial, circumferential, and radial coordinates, respectively. The cylindrical coordinates in the nondeformed state is designated by t, φ, , and r, respectively (the reference system of coordinates). Along with the radial coordinate r, we also use the normal coordinate $z = r - a$. The problem was solved according to the conditions of macroscopically axisymmetric deformation of a cylinder, when the macrocoordinate angles $\hat{\omega}_{12} = \hat{\omega}_{23} = \pi / 2$. The numerical schemes of the macro- and micromechanical levels of analysis are similar to the corresponding ones of the problem on reduction by pressure of a rectangular prism.

Figure 4 also shows configurations of a reinforced material block of the prism in the initial state and in the deformed configuration at $\hat{p} = 9$ MPa. These configurations are valid for the block with coordinates of its geometrical center t = 20 mm and z = 20 mm (as well as for the block with coordinates t = l – 20 mm = 380 mm and z = 20 mm). For the given block, the rectangular (quasi-rectangular) packing of fibers is determined by the ratio of sides of a rectangular package directed along the radial and circumferential directions as 1:1.1. The deformed configuration of the block at such loading of the prism is characterized by the axial, circumferential, and radial elongation ratios $\hat{\lambda}_1$ = 1.013, $\hat{\lambda}_2$ = 1.059, and $\hat{\lambda}_3$ = 0.683, respectively, and the coordinate angle $\hat{\omega}_{13}$ = 71.3 deg. The cross section of the fiber in the deformed ("Euler") block is characterized by the ratio $\hat{d}_{\rm fa} / \hat{d}_{\rm fb}$ = 0.737 mm/0.571 mm = 1.291. The stretch ratio of the axial line of a fiber is $\hat{\lambda}_{\rm f} = \hat{\lambda}_1$ = 1.013.

Figure 5 presents the reference configuration of the cylinder and its configurations at $\hat{p}$ = 9 MPa, calculated by the carcass and applied theories. The displacements of the outer surface $r = b$ found by the carcass theory considerably exceed those of the inner one $r = a$, with $\hat{u}_{(3)a}$ = –1.7 mm and $\hat{u}_{(3)b}$ = –64.4 mm for the central cross section. The central displacements of surfaces according to the applied theory also considerably differ: $\hat{u}_{(3)a}$ = 19.1 mm and $\hat{u}_{(3)b}$ = –74.5 mm. A qualitative distinction between displacement patterns obtained by the carcass and applied theories lies in the fact that radial displacements of the inner and outer surfaces of the cylinder by the applied theory are always directed toward each other. According

to the carcass theory, the external pressure acting on the outer surface of the cylinder "presses through" the inner surface at its central part. This is explained by account of the effect of finite cross sections of fibers on displacements of the prism.

Figure 6 shows the central deflections of face surfaces of the cylinder as functions of the reduction pressure calculated on the basis of carcass theory. In the central part of the inner surface $r = a$, the radial displacements occur in the direction toward the cylinder axis on the whole interval $0 \le \hat{p} \le 9$ MPa. The greatest-in-magnitude value of the central deflection of the given surface $\hat{u}_{(3)a} = -8.2$ mm is reached at $\hat{p} = 5.5$ MPa. In this case, the central deflection of the outer surface is $\hat{u}_{(3)b} = -44.6$ mm. Thus, we have to conclude that, at high values of fiber content, the applied theory yields significant errors in calculating the reduction pressure for reinforced bodies both at large and small deformations.

Conclusions

A comparison of the results obtained on the basis of both theories demonstrates that the compression of reinforced bodies with a high content of fibers, when distances between the fibers considerably decrease, cannot be investigated by using the applied theory. In such cases, an extreme loading of the material of reinforced body occurs, when the greatest changes of material lengths in it are oriented mainly across fibers. Such a type of deformation of a body must be investigated by using the carcass theory. A similar situation occurs in deformation increasing the distance between fibers, as in the problem solved earlier, on the butt-end torsion of a cylinder with the axial arrangement of fibers.

REFERENCES

1. V. M. Akhundov, "Modeling large deformations of fibrous bodies of revolution based on applied and carcass theories. 1. Butt-end torsion of cylindrical and toroidal вodies," Mech. Compos. Mater., **50**, No. 2, 245-256 (2014).
2. V. M. Akhundov, "Applied theory of composites with a small content of fibers under large deformations," Mech. Compos. Mater. Struct., **7**, No. 1, 3-15 (2001).
3. V. M. Akhundov, "Structural macroscopic theory of stiff and soft composites. Invariant description," Mech. Compos. Mater., **34**, No. 5, 419-432 (1998).
4. V. M. Akhundov, "Carcass theory of stiff and soft composites with uncurved and curved structures. Invariant description," Mech. Compos. Mater. Struct., **6**, No. 2, 275-293 (2000).
5. N. S. Bakhvalov, N. P. Zhidkov, and G. M. Kobel'kov, Numerical Methods [in Russian], Nauka, Moscow (1987).
6. F. L. Chernous'ko and V. P. Banichuk, Variational Problems of Mechanics and Control [in Russian], Nauka, Moscow (1973).
7. A. S. Sakharov and I. Altenbach (eds.), Finite-Element Method in the Mechanics of Solid Bodies [in Russian], Vishcha Shkola, Kiev (1982).
8. R. P. Fedorenko, Approximate Solution of Problems of Optimum Control [in Russian], Nauka, Moscow (1978).
9. M. Levinson and I. W. Burgess, "A comparison of some simple constitutive relations for slightly compressible rubber-like materials," Int. J. Mech. Sci., **13**, 563-572 (1971).
10. P. J. Blatz, Application of Finite Elastic Theory in Predicting the Performance of Solid Propellant Rocket Motors, Calif. Inst. Techn. GALCJISM (1960), pp. 60-125.
11. V. A. Kabanov et al. (eds), Encyclopedia of Polymers, Vol. 3 [in Russian], Sovets. Entsikl., Moscow (1977).
12. V. M. Akhundov, "Analysis of elastomeric composites based on fiber-reinforced systems. 2. Unidirectional composites," Mech. Compos. Mater., **35**, No. 1, 19-32 (1999).